A Numerical Solution for the Transient Displacement of a Circumferentially Moving Cylindrical Shell

S. Müftü
Student Mem. ASME

R. C. Benson
Mem. ASME

Mechanics of Flexible Structures Project,
Department of Mechanical Engineering,
University of Rochester,
Rochester, NY 14627

In magnetic tape recording it is important to control the tape displacement as it is transported over guides and recording heads. In this paper a numerical solution is presented for the transient motion of a tape that is circumferentially transported. The tape may be modelled as a thin cylindrical shell, with "gyroscopic" effects arising from the tape transport. Spatial derivatives are discretized with finite difference approximations, and time derivatives are discretized by Newmark's method. The result is a robust computer algorithm that is used in making 3D-transient simulations of flexural waves following a radial load. This ability is demonstrated to be important for realizing that reflection of the waves from the lateral sides of the tape has significant effect on the transient displacement. Results that have been previously published on "critical" speeds, wave shapes near a concentrated load point, and the dominant period of the load point displacement are further developed. A better approximation of the critical tape speed is presented, and the dominant period of the load point displacement is found to be dependent on the tape velocity.

1 Introduction

In magnetic recording applications, controlling the tape displacement over a read-write head is an important design consideration for the quality of the magnetic signal. This issue is especially important in helical scan recording in which a read-write head travels relative to the tape with high velocity and causes intermittent loading on the tape. This loading, in turn, causes a transient displacement pattern in the tape.

Bogy et al. (1974), and Nishida and Hosaka (1984) among others, modeled the tape as a cylindrical shell, and computed the steady state tape displacements due to a point load. They have concluded that above a "critical" speed the wavelength of the standing wave is smaller upstream of the load in comparison with the wavelength downstream the load. Ono and Ebihara (1984) generalized the solution methods for the same problem. Sundaram and Benson (1990) solved the transient equations of motion, and investigated the displacements in the cylindrical shell in response to a point load in space applied as a step function in time. Each of these studies represent the tape displacement with infinite series that require calculation of a great number of modes for convergence. The standing wave pattern that is predicted by Bogy et al. (1974), and Nishida and Hosaka (1984) were qualitatively and experimentally verified by Albrecht et al. (1977), Feliss and Talke (1977), and Lacey and Talke (1990).

There are few analyses for transient displacement in a circumferentially moving medium. One exception is Wickert and Mote (1990) who studied a traveling string (a spatially one dimensional tape) and showed that mode shapes are nonsymmetric when a "gyroscopic" effect is included. This effect vanishes when the tape transport velocity is zero.

In this paper a numerical approach to the solution of transient motion of a cylindrical shell, that is circumferentially transported, is presented. The equations of motion are discretized by using finite differences in the space domain and Newmark's method (Newmark, 1952) in the time domain. This numerical procedure proves to be very efficient, thus allowing for a detailed investigation of various kinds of loadings. In order to make comparisons with the existing literature, a moving tape's response to a concentrated load is investigated. With this method the wave action in the tape is easily followed by making time history plots consisting of three-dimensional (3D) "wire frame" drawings. This investigation showed that the continuous reflection and superposition of waves from the *lateral* edges of the tape contribute significantly to the displacement of the load joint. We were able to find similar results as the previous studies, on critical tape speed, and dominant period of the displacement at the load point. Moreover, we found that this dominant period is a function of the tape transport velocity. We also confirmed the dispersive nature of the wave behavior, hence making it impossible to observe a single wave speed. Nevertheless, our time history plots allow for determination of an *apparent* wave speed.

Contributed by the Technical Committee on Vibration and Sound for publication in the JOURNAL OF VIBRATION AND ACOUSTICS. Manuscript received Oct. 1992; revised Sept. 1993. Associate Technical Editor: L. A. Bergman.

Table 1 Variables and typical values for a magnetic recording application

D	Bending rigidity	$(=\frac{Ec^3}{12(1-\nu^2)})$	$2.9\text{x}10^{-6} Nm$
k	Shell stiffness	$(=\frac{Ec}{R^2(1-\nu^2)})$	$219.8\text{x}10^{6} N/m^3$
E	Young's Modulus		$4\text{x}10^{9}$Pa
ν	Poisson's ratio		0.3
ρ_a	Shell density per unit area		$0.014\ kg/m^2$
R	Radius of the shell		$2\text{x}10^{-2} m$
c	Shell thickness		$20\text{x}10^{-6} m$
$\frac{T_x}{R}$	Belt wrap pressure		$4500 Pa$
T_x	Tension per unit length		$90 N/m$
L_y	Width of the tape		$6.35\text{x}10^{-3} m$
L_x	Length of the tape		$4L_y$ or $19L_y$
P_o	Concentrated load Magnitude		200 Pa
$\Delta x = \Delta y$	Spatial Step		$1.549\text{x}10^{-4} m$
dt	Time Step		$2\text{x}10^{-6}$ s
β	Parameter for Newmark's Method		1/4
γ	Parameter for Newmark's Method		1/2

2 Equation of Motion

The equation governing the radial displacements, $w(x, y)$, of a cylindrical shell subject to static radial loading, $P(x, y)$ and a constant circumferential tension, T_x, is given by Timoshenko and Gere (1988). The inertial forces, $\rho_a D^2w/Dt^2$, can be added to this equation by virtue of d'Alembert's principle. Here the material time derivative

$$\frac{D(.)}{Dt}=\frac{\partial(.)}{\partial t}+V_x\frac{\partial(.)}{\partial x} \tag{1}$$

is used in order to properly account for tape transport effects (Wickert and Mote, 1990). In this equation we assume that the tape transport is only in the circumferential direction, with velocity, V_x. With this adjustment the equation of motion of the tape becomes,

$$D\nabla^4 w+(\rho_a V_x^2-T_x)\frac{\partial^2 w}{\partial x^2}+kw+2\rho_a V_x\frac{\partial^2 w}{\partial x\partial t}+\rho_a\frac{\partial^2 w}{\partial t^2}=\mathrm{P(x,\ y,\ t)}-\frac{T_x}{R} \tag{2}$$

The variables of this equation along with nominal values are given in Table 1.

The boundary conditions of the tape are such that it is "simply supported" along two lines running across the tape and "free" along its lateral edges. See Fig. 1. The boundary conditions and the initial conditions are as follows,

Simply Supported Sides:

Zero Moment for $x = 0$, L_x, and $0 \le y \le L_y$

$$D\left[\frac{\partial^2 w}{\partial x^2}+\nu\frac{\partial^2 w}{\partial y^2}\right]=0 \tag{3}$$

Zero Displacement for $x = 0$, L_x, and $0 \le y \le L_y$

$$w=0 \tag{4}$$

Free Edges:

Zero Moment for $y = 0$, L_y, and $0 \le x \le L_x$

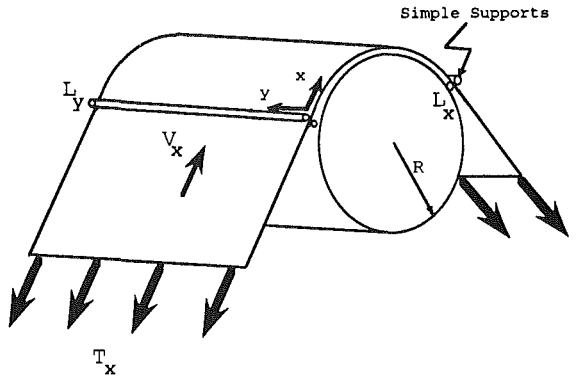

Fig. 1 The geometry of the tape

$$D\left[\frac{\partial^2 w}{\partial y^2}+\nu\frac{\partial^2 w}{\partial x^2}\right]=0 \tag{5}$$

Zero Equivalent Shear Force for $y = 0$, L_y, and $0 \le x \le L_x$

$$D\left[\frac{\partial^3 w}{\partial y^3}+(2-\nu)\frac{\partial^3 w}{\partial x^2 y}\right]=0 \tag{6}$$

Initial Conditions:

Initial Displacement for $t = 0$

$$w(x, y, 0)=w^o(x, y) \tag{7}$$

Initial Displacement Velocity for $t = 0$

$$\frac{\partial w(x, y, 0)}{\partial t}=v^o(x, y) \tag{8}$$

Here, w^o, v^o are two spatial functions to be defined. The spatial derivatives of Eq. (2) are discretized by using central finite difference approximates of the derivatives. As the boundary conditions of the problem are independent of time, Eqs. (3–6) are similarly discretized. This procedure (Timoshenko and Woinkowsky-Kreiger, 1987) transforms the continuous Eqs. (2–6) to a discretized form in space which can be represented in a matrix notation as follows,

$$[K]\{\mathbf{w}\}+[G]\{\mathbf{v}\}+[M]\{\mathbf{a}\}=\{\mathbf{P}\} \tag{9}$$

where

- [K] is a stiffness matrix
- [G] is a matrix that contains the "gyroscopic" terms
- [M] is a diagonal mass matrix
- {P} is a discretized load vector
- {w} is a discretized displacement vector
- {v} is a discretized velocity vector of w's $\left(=\frac{\partial\{w\}}{\partial t}\right)$
- {a} is a discretized acceleration vector of w's $\left(=\frac{\partial^2\{w\}}{\partial t^2}\right)$

Equation (9) is discretized in time with equal time steps, Δt, by using a "displacement form" of the Newmark's method (Newmark, 1952). In the discretized time domain the current time step is indicated by the superscript n, and the next one is indicated by $n + 1$. This method "marches" in the discrete time domain by using the following steps;

(*1*) Predict displacement and velocity vectors by,

$$\{\tilde{\mathbf{w}}\}^{n+1}=\{\mathbf{w}\}^n+\Delta t\{\mathbf{v}\}^n+\left(\frac{1}{2}-\beta\right)\Delta t^2\{\mathbf{a}\}^n \tag{10}$$

$$\{\tilde{\mathbf{v}}\}^{n+1}=\{\mathbf{v}\}^n+(1-\gamma)\Delta t\{\mathbf{a}\}^n \tag{11}$$

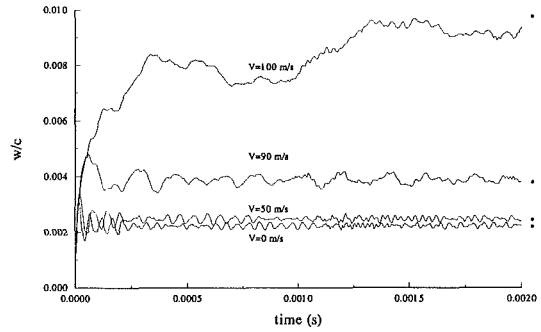

Fig. 2 Transient displacement of the load point ($x = L_x/2$, $y_o = L_y/2$) for a concentrated step load as a function of tape velocities, (0, 50, 90, 100 m/s), $L_x/L_y = 19$. Dots indicate steady state deflections.

If $n = 0$ then use the initial conditions $\{\mathbf{w}\}^o$, and $\{\mathbf{v}\}^o$.

(*2*) Obtain the displacement vector at time $n + 1$, by solving

$$[K]_{eq}\{\mathbf{w}\}^{n+1} = \{\mathbf{f}\}_{eq}^{n+1} \tag{12}$$

(*3*) Calculate the acceleration and velocity vectors at time $n + 1$, by

$$\{\mathbf{a}\}^{n+1} = \frac{1}{\beta\Delta t^2}\left(\{\mathbf{w}\}^{n+1} - \{\tilde{\mathbf{w}}\}^{n+1}\right) \tag{13}$$

$$\{\mathbf{v}\}^{n+1} = \{\tilde{\mathbf{v}}\}^{n+1} + \gamma\Delta t\{\mathbf{a}\}^{n+1} \tag{14}$$

(*4*) Increment time by Δt, let $n + 1 \rightarrow n$, and go to Step 1.

In the preceding $[K]_{eq}$ and $\{\mathbf{f}\}_{eq}$ are given by the following expressions,

$$[K]_{eq} = [[M] + \gamma\Delta t[G] + \beta\Delta t^2[K]] \tag{15}$$

$$\{\mathbf{f}\}_{eq}^{n+1} = \beta\Delta t^2\{\mathbf{f}\}^{n+1} + [M]\{\tilde{\mathbf{w}}\}^{n+1} - \beta\Delta t^2[G] \times \left[\{\tilde{\mathbf{v}}\}^{n+1} - \frac{\gamma}{\beta\Delta t}\{\tilde{\mathbf{w}}\}^{n+1}\right] \tag{16}$$

The intermediate variables $\{\tilde{\mathbf{w}}\}$, $\{\tilde{\mathbf{v}}\}$ of Step 1, are called "predictors," β and γ are two parameters related to Newmark's method. Because the equivalent stiffness matrix in Eq. (12) does not change with time, the solution requires only one "inversion" of this matrix before the time marching scheme is initiated.

By choosing different values for parameters, β and γ it is possible to introduce numerical damping to the solution. In general, γ controls the numerical damping and consistency of the truncation error throughout the solution. With appropriate choice of γ, the parameter β is used in controlling stability, and amplitude and period errors of the solution. A choice of $\beta = 1/4$ and $\gamma = 1/2$ provides an unconditionally stable algorithm without any algorithmic damping. On the other hand, the case of $\beta = 1$ and $\gamma = 3/2$ has strong damping characteristics and can be used to quickly bring a transient solution to static equilibrium (Hughes, 1987).

3 Results and Discussion

We developed a computer program for the solution method that is outlined above, and analyzed the tape's response to an external loading of the following type,

$$P = P_o e^{-\alpha(x-x_o)^2} e^{-\alpha(y-y_o)^2} H(t) \tag{17}$$

where, x_o and y_o mark the centroid of the load, and $H(t)$ is the Heaviside step function. The centroid of the load will be referred to as the "load point" hereafter. The tape was initially in static equilibrium, i.e. $w^o = 0$ and $v^o = 0$. The exponential function in Eq. (17) is chosen to approximate a concentrated load. The parameter α is adjusted so that the function decays to 1 percent of its maximum, within a decay distance of 5 percent of L_y from the load point. In order to demonstrate the applicability of the method we show results for two cases with different length-to-width ratios, $L_x/L_y = 4$ and 19. All of the figures in this paper are obtained using the specifications given in Table 1. The cases with the smaller L_x/L_y were run on a computer workstation. Roughly 20 minutes were required to complete 250 time steps.

In Fig. 2, the transient response of the load point is plotted for $V_x = 0$, 50, 90 and 100 m/s. The load is located at the center of the tape, ($x_o = L_x/2$, $y_o = L_y/2$). The length-to-width ratio is 19. In order to choose the time step we performed numerical experiments in the range $0.5\ \mu s \le \Delta t \le 12.5\ \mu s$, on a spatial mesh with $\Delta x = \Delta y = 1.549 \times 10^{-3}$ m. We chose the largest possible time step, $\Delta t = 2\ \mu s$, that did not cause an appreciable difference in the time history of the load point.

We note from Fig. 2 that at lower tape speeds, the tape motion consists of the superposition of several modes with one dominant period. For the case of $V_x = 0$ the dominant period is close to $2\pi(\rho_a/k)^{1/2}$, which is approximately 50 μs for the specifications of this problem. We also note that the displacement of the tape decays within an envelope that asymptotes at a finite amplitude. As Eq. (2) does not have a dissipative term* the tape displacement will asymptote on a quasi-periodic motion around a steady state value. Similar observations were also made by Sundaram and Benson (1990). The dots on Fig. 2 indicate the nondimensional displacements at steady state. These values were separately obtained by running the program with Newmark parameters $\beta = 1$ and $\gamma = 3/2$. The steady state values obtained in this way match the static solution of Eq. (2).

Furthermore, from Fig. 2, we observe that the dominant period and the mean displacement increases as the velocity of the tape is increased. These increases are nonlinear functions of velocity, and a very large change is observed near $V_x = 100$ m/s. Increasing tape transport velocity has an effect of reducing the effective tape tension, $T_{eff} = T_x - \rho_a V_x^2$. See Eq. (2). At the transport speed,

$$V_x = \sqrt{\frac{T_x}{\rho_a}} \tag{18}$$

the effective tape tension vanishes. At tape transport speeds above this value T_{eff} becomes compressive, and the tape becomes prone to *buckling*. However, the shell stiffness, k, acts as a spring foundation and prevents the immediate appearance of buckling. As the tape transport speed is increased, the in-plane compression created by the effective tension can no longer be counteracted by the resisting effect of the shell stiffness and unbounded displacements occur. The speed at which this phenomenon occurs is called the "critical" tape speed.

We have found that for the parameters used in this paper, a small positive change in the transport speed from the value $V_x = 100$ m/s causes the unbounded displacements. This value lies between the values calculated by using the approximate critical tape speed expressions that are derived by Wickert and Mote (1990), (80 m/s), and Sundaram and Benson (1989), (111 m/s). The difference can be explained as follows; in Wickert and Mote (1990), the expression for the critical tape speed is derived for an axially moving beam, hence the shell stiffness term does not play a role which explains the reason for a lower bound approximation. In Sundaram and Benson (1989), on the other hand, the expression for the critical tape speed is derived for a cylindrical shell that is simply supported on all of its sides. In our study the tape is modeled as having two free edges, which simulates a structure which would have lesser resistance to buckling loads. Therefore, we find it natural to

* The displacement decay is due to dispersion.

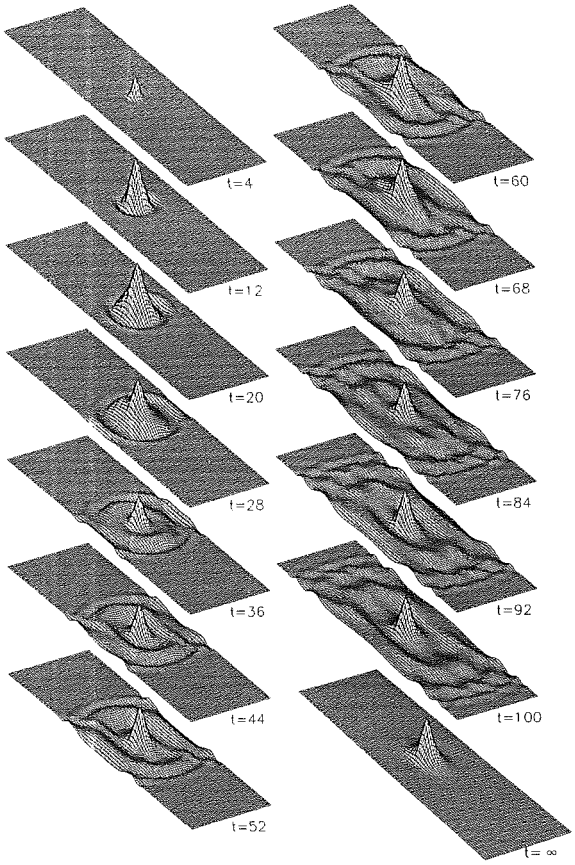

Fig. 3 Displacement wave propagation of the tape in response to a concentrated step load, V_x = 0 m/s, L_x/L_y = 4, (time in μs—tape motion from upper-left to lower right)

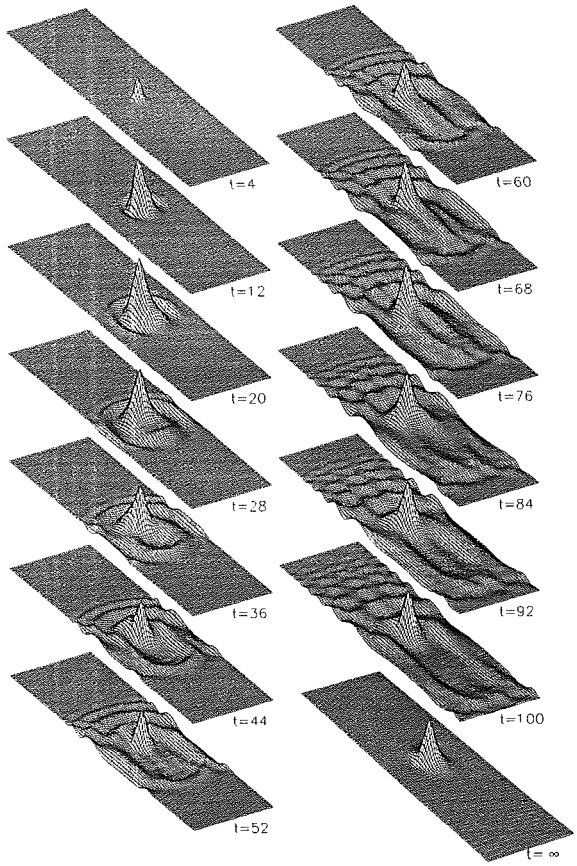

Fig. 4 Displacement wave propagation of the tape in response to a concentrated step load, V_x = 50 m/s, L_x/L_y = 4, (time in μs—tape motion from upper-left to lower right)

observe a critical tape speed less than that given by Sundaram and Benson (1989), and greater than that given by Wickert and Mote (1990).

Figures 3 and 4 show 3D wire frame time history plots of a tape with $L_x/L_y = 4$, and two choices of tape transport velocity, $V_x = 0$ and 50 m/s. In these two figures, the pictures that are labeled as $t = \infty$ are the steady state displacements obtained with $\beta = 1$ and *gamma* = 3/2. The rest of the pictures are obtained with $\beta = 1/4$ and $\gamma = 1/2$ and represent the transient response. These figures show that load causes displacements waves. When $V_x = 0$, waves propagate radially away from the load point, and are symmetrical with respect to the $x = L_x/2$ line. Due to applied tension, the tent-like shape of the displaced tape has an ellipsoidal "footprint" whose major axis is aligned with the tensioned direction.

The waves that reflect from the free edges travel back toward the source. From Figs. 3 and 4, it can be observed that first wave reflection from the free edges occurs near time $t = 28$ μs. By the time the forward travelling wave front reaches the simply supported edge, several side-to-side wave interactions have already occurred. We believe that the wave reflection from the free edges explains the major reason for the nonperiodic behavior of the load point in Fig. 2.

Figure 4 demonstrates the effect of the tape transport velocity (V_x = 50 m/s) on the wave profiles. In this figure we see that the wavelength of the displacement is larger downstream of the load, than upstream of the load. This was also predicted by the steady state analysis of Bogy et al. (1974) and observed experimentally by Lacey and Talke (1990) among other investigators.

Comparison of Fig. 3 to Fig. 4 shows that the wave front travelling toward the support on the downstream side of the tape has a shorter travel time when the tape transport speed is increased. However, numerical simulations showed that determination of the wave speed is not straight forward. As the governing equation is *dispersive* in nature (Kevorkian, 1990), wave fronts with small wavelengths reach the simply supported boundaries in a shorter time than the ones with longer wavelengths. We are able to visually detect only a simple dominant wave front by looking at Figs 3–6.

Figures 5 and 6 show the wave propagation on the longer tape, $L_x/L_y = 19$, at its middle cross section in the y-direction, $y = L_y/2$. The tape transport velocities are $V_x = 50$ and 100 m/s. In these figures the whole length, L_x, of the tape is shown on the horizontal axis. The vertical axes are magnified 5.9×10^6 times in Fig. 5 and 1.5×10^6 times in Fig. 6. As in previous figures, these also show that the wavelength of the displacement is larger downstream of the load. For both velocity cases the displacement near the load point becomes nearly constant within 800 μs after the application of the load. The same observation can be made on the 3D wire frame pictures as well.

Figures 5 and 6 help to better understand the behavior of the waves that are reflected from the simply supported boundaries. A type of "Doppler effect" is observed as the waves that are reflected from the simply supported boundary at the right travel back toward the load point with smaller wavelengths. Waves that reflect from the left-side boundary acquire larger wavelengths. Comparing the behavior upstream of the load in Figs. 5 and 6 it is seen that, when the tape transport speed is close to critical, little energy reaches the left-hand boundary through backward travelling waves. As the governing Eq. (2) is dispersive, we expect short wavelength, high speed waves to reach the left-hand side support. In fact, the picture

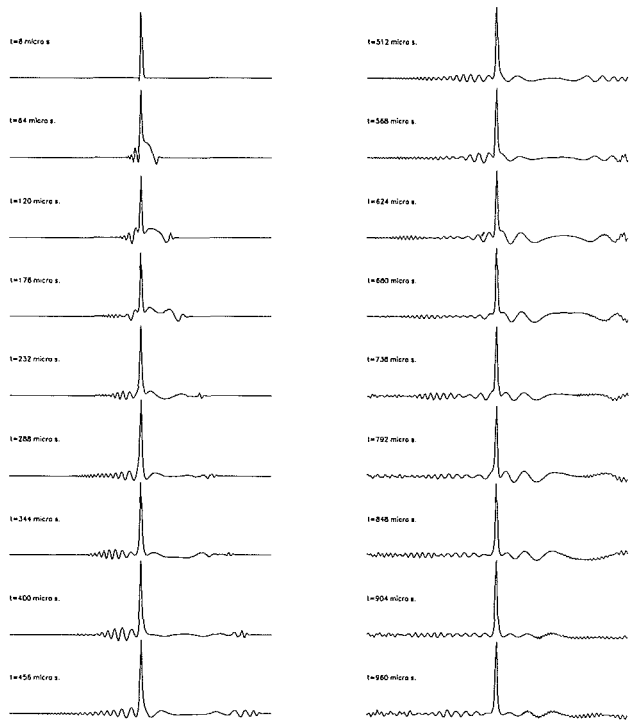

Fig. 5 Wave action at the $y = L_y/2$ cross-section in response to a concentrated step load, $V_x = 50$ m/s, $L_x/L_y = 19$ (tape movement from left to right)

labeled $t = 736$ μs in Fig. 6 shows a reflection of minute amplitude.

4 Conclusions

We produced an efficient numerical method for the solution of the transient displacements of a cylindrical shell. The equations of motion include the "gyroscopic" term. The method involves finite differences in the spatial domain and Newmark's method in the time domain. Due to the computing efficiency it is easy to obtain the time history of the wave action in 3D plots. We considered the fact that the tape has finite width, and studied its influence on the displacement behavior in response to a localized step load. This enabled us to show that the wave front that propagates in the width (or axial) direction has a substantial effect on the displacement behavior of the load point. As this wave is reflected from the free edge, it contributes to the displacement amplitude of the load point which eventually settles into an *envelope* over time. We concluded that the reason for the irregular load point displacements within this envelope is the continuous superposition of many waves that reflect from the free lateral edges of the tape. We confirmed the observations in Sundaram and Benson (1990) that the load point displacement, however irregular looking, has a dominant period, which is approximated to $2\pi(\rho_a/k)^{1/2}$ for $V_x = 0$. This period is found to increase with increasing tape transport speed.

We also observed a critical tape transport speed that was predicted by other investigators. However, since we modeled the lateral sides of the tape as free edges, we were able to evaluate the critical tape transport speed closer to its actual value than predicted by alternative models with different boundary conditions.

The general behavior of the wavelength that we found (short waves lengths upstream of the load and larger ones downstream) compares qualitatively with prior analysis for steady state systems. Moreover, we observed that the waves generated

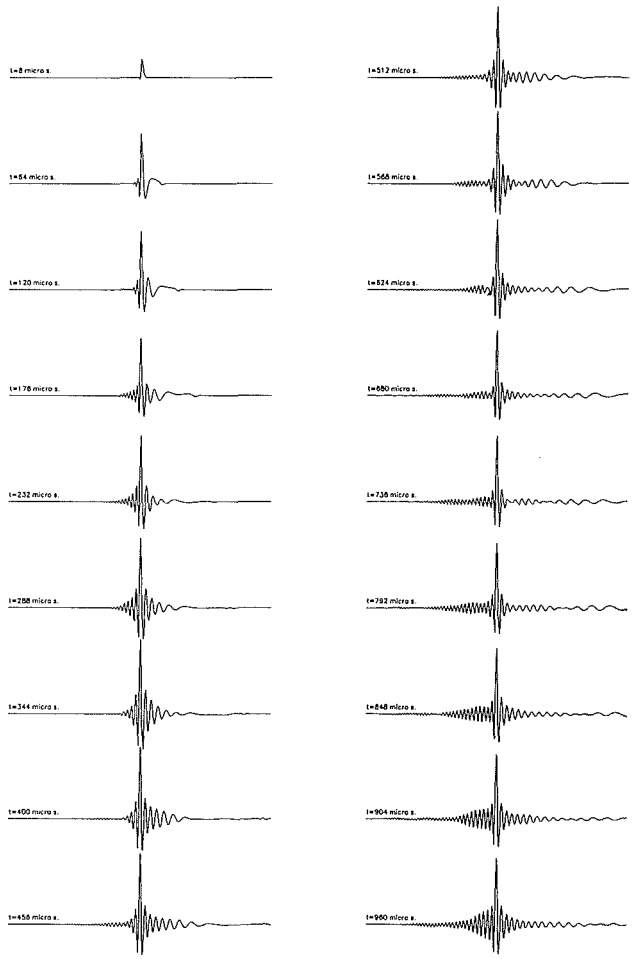

Fig. 6 Wave action at the $y = L_y/2$ cross-section in response to a concentrated step load, $V_x = 100$ m/s, $L_x/L_y = 19$ (tape movement from left to right)

by the localized load that we used are dispersive and only an apparent wave front can be detected. We also found that the tape displacement settles to a near steady state shape with small reflected waves superimposed onto this.

Currently the authors are working on parameter studies of this problem (Müftü and Benson, 1993), as well as coupling this method with a Reynolds equation solver, in order to reach a fully coupled transient solution to the air lubricated foil bearing problem (Gross, 1980).

5 Acknowledgment

Supercomputer time that has been provided by the Cornell Theory Center, Cornell National Supercomputer Facility is gratefully acknowledged.

References

Albrecht, D. M., Laenen, E. G., and Lin, C., 1977, "Experiments on the Dynamic Response of a Flexible Strip to Moving Loads," *IBM Journal of Research and Development*, pp. 397–383.

Bogy, D. B., Greenberg, H. J., and Talke, F. E., 1974, "Steady Solution for Circumferentially Moving Loads on Cylindrical Shells," *IBM Journal of Research and Development*, Vol. 18, pp. 395–400.

Feliss, N. A., and Talke, F. E., 1977, "Capacitance Probe Study of Rotating-Head/Tape Interface," *IBM Journal of Research and Development*, pp. 289–293.

Gross, W. A., ed., 1980, *Fluid Film Lubrication*, Wiley-Interscience, NY, pp. 482–501.

Hughes, T. J. R., 1987, *The Finite Element Method: Linear Static and Dynamic Finite Element Analysis*, Prentice-Hall, NJ, pp. 490–567.

Kevorkian, J., 1990, *Partial Differential Equations*, Wadsworth & Brooks/Cole, Pacific Grove, CA., pp. 170–178.

Lacey, C. A., and Talke, F. E., 1990, "Tape Dynamics in a High-Speed Helical Recorder," *IEEE Transactions on Magnetics*, Vol. 26, pp. 2208–2210.

Müftü, S., and Benson, R. C., 1993, "Numerical Simulation of Tape Dynamics in Helical Scan Recording," *IEEE Intermag-93 Conference Digest, GD-09*, Stockholm, Sweden.

Newmark, N. M., 1952, "Computation of Dynamic Structural Response in the Range Approaching Failure," *Proc. of the Symposium on Earthquake and Blast Effects on Structures: Los Angeles, CA*, June, pp. 114–129.

Nishida, Y., and Hosaka, H., 1984, "Dynamic Deflection of Magnetic Tape Due To Rotating Head Scanning," *Bulletin of the JSME*, Vol. 29, No. 256, pp. 3530–3537.

Ono, K., and Ebihara, T., 1984, "Improved Green's Function in Tape Deflection and Solutions of Head Contour with Uniform Contact Pressure," *Tribology and Mechanics of Magnetic Storage Systems, SP-16*, pp. 97–102.

Sundaram, R., and Benson, R. C., 1989, "A Green's Function with Improved Convergence For Cylindrically Wrapped Tapes," *Tribology and Mechanics of Magnetic Storage Systems, STLE, SP-26*, pp. 98–110.

Sundaram, R., and Benson, R. C., 1990, "Tape Dynamics Following An Impact," *IEEE Transactions on Magnetics*, Vol. 26, pp. 2211–2213.

Timoshenko, S. P., and Gere, J. M., 1988, *Theory of Elastic Stability*, McGraw-Hill, New York, pp. 440–453.

Timoshenko, S. P., and Woinkowsky-Kreiger, S., 1987, *Theory of Plates and Shells*, McGraw-Hill, New York, pp. 351–363.

Wickert, J. A., and Mote, C. D., Jr., 1990, "Classical Vibration Analysis of Axially Moving Continua," ASME *Journal of Applied Mechanics*, Vol. 57, pp. 738–744.